Theoretical Study of the Mechanism of Thermal Decarboxylation of Salicylic and *p*-Aminobenzoic Acids; Models for Aqueous Solution

Paul Ruelle
School of Pharmacy, University of Lausanne, 3 Place du Château, CH-1005 Lausanne, Switzerland

The mechanism of decarboxylation of salicylic and *p*-aminobenzoic acids in aqueous solution has been investigated by *ab initio* methods using the STO-3G basis set and fully optimized geometries. Single-point 3-21G energy calculations were then performed to improve the results. The mechanism suggested is a pseudo-unimolecular concerted decomposition of the free acid by interaction with a chain of water molecules, the α-protonated form of the carboxylate anion representing the activated complex. In comparison with unsubstituted benzoic acid, the presence of *ortho*- and *para*-electron-releasing groups increases the electron density at the carbon atom next to the carboxy group, hence facilitating the approach of the electrophilic proton, and decreasing the activation energy.

Thermal decarboxylation is frequently used in both degradative and synthetic procedures and in enzymic reactions. Its nature has been established [1–4] as that of an electrophilic substitution reaction, which may occur by two different mechanisms. For carboxylic acids containing strongly electron-withdrawing substituents, *e.g.* cyanoacetic acid [5] or 2,4,6-trinitrobenzoic acid,[6] loss of carbon dioxide occurs in the unimolecular rate-determining step and is followed by rapid protonation of the intermediate carbanion [S_E1 mechanism (i)].

$$\begin{array}{ll} & RCO_2H \rightleftharpoons R^- + CO_2 + H^+ \\ S_E1 & \\ & R^- + H^+ \longrightarrow RH \end{array} \quad \text{(i)}$$

On the other hand, carboxylic acids having electron-donating substituents, *e.g.* hydroxybenzoic acids,[1] seem to undergo decarboxylation according to a bimolecular rate-determining reaction involving the attack of a proton, or a protonated solvent, at the carbon atom next to the carboxy group. This first step is followed by the loss of carbon dioxide from the unstable σ-complex thus formed [S_E2 mechanism (ii)].

$$\begin{array}{ll} & RCO_2H + H^+ \rightleftharpoons HRCO_2H^+ \quad (\sigma\text{-complex}) \\ S_E2 & \\ & HRCO_2H^+ \longrightarrow RH + CO_2 + H^+ \end{array} \quad \text{(ii)}$$

However, when one attempts to establish either decarboxylation mechanism from kinetic experiments, the first problem which arises is to discover whether the substrate undergoes decarboxylation as a free acid [as indicated in equations (i) and (ii)], or as a carboxylate anion, or even as a zwitterion. The position of the proton at the moment of the decarboxylation remains to be determined. Moreover, in the case of a postulated S_E2 mechanism, the second problem which arises is whether the α-protonated form (the σ-complex) should be considered as a true reaction intermediate or as a transition state. In other words, because no definitive experimental evidence for the existence of such intermediates is available, it is not clear whether the protonation and the departure of carbon dioxide are sequential (as shown) or concerted. The concerted mechanism would involve the introduction of the proton and the breaking of the carbon–carbon bond in a single step.[7–9]

To gain a better understanding of the thermal decarboxylation of aromatic carboxylic acids in solution, *ab initio* theoretical studies have recently been performed on the decomposition of acrylic and benzoic acids in aqueous solution.[10] The results delineated a concerted mechanism including, at the transition state, the presence of two water molecules, the active participation of which led to a significant catalytic effect. In order to obtain more insight into this mechanism, as well as to emphasize the substituent effect of *ortho*- and *para*-electron-releasing groups, theoretical investigations have now been carried out on the decarboxylation of salicylic and *p*-aminobenzoic acids in aqueous solution. Again, in these reactions, the solvent has been considered not merely as a continuum medium (solvation effects are not taken into account), but as an active participant.

Methods

To describe the mechanism of the two reactions, *ab initio* molecular-orbital calculations were performed using the MONSTERGAUSS program [11] with a CDC CYBER 180/855 computer. Analytical gradient-optimization procedures were used with the STO-3G basis set [12] to locate the stationary points on the reaction energy hypersurfaces. The geometry optimizations were carried out for all geometrical parameters. The transition states were located by minimizing the gradient norm while ensuring that the matrix of the second derivatives of the energy had only one negative eigenvalue. The Hessian matrices were computed by gradient differences by the VA05AD method.[13] In order to improve the results, the STO-3G-optimized geometries were then used for a single-point energy calculations with the split-valence 3-21G basis set [14] (denoted 3-21G//STO-3G in the text).

Results and Discussion

Carboxylic acids lose carbon dioxide under a variety of experimental conditions. Kinetic data on the decarboxylation of *p*-aminobenzoic acid both in aqueous solution at temperatures below 80 °C,[15–17] and in glycerol [18] and catechol [19] at temperatures above 160 °C have been reported. On the other hand, all kinetic work dealing with the thermal decomposition of salicylic acid has been carried out in non-aqueous solvents between 160 and 250 °C,[2,20–22] or in the molten state between 160 and 180 °C.[23] However, for convenience, in this article emphasis will be given to decarboxylation in aqueous solution, the solvent being represented, in the supermolecular approach, successively by one and two water molecules.

For each reaction considered here, six stationary points have been located on the relevant energy hypersurfaces: the reactant (salicylic or *p*-aminobenzoic acid), three transition states (a four-, a six-, and an eight-centre transition state corresponding, respectively to no catalysis, catalysis by one water molecule, and catalysis by two water molecules), and two product molecules (phenol or aniline and carbon dioxide). The values of the

geometrical parameters which undergo the largest modifications along the reaction pathway, as well as the structures of all these stationary points (except CO_2), are given in Tables 1—5 and Figures 1—5

Table 1. STO-3G-optimized geometrical parameters of salicylic acid (SA) and *p*-aminobenzoic acid (PABA) (bond lengths in Å; bond and torsion angles in degrees)

Parameter	SA	PABA	Parameter	SA	PABA
C(1)–C(2)	1.499	1.511	*d*	1.376	1.381
C(2)–O(3)	1.232	1.220	C(1)–C(2)–O(3)	123.9	125.9
C(2)–O(4)	1.382	1.393	C(1)–C(2)–O(4)	114.8	112.9
O(4)–H(5)	0.990	0.989	C(2)–O(4)–H(5)	104.6	104.2
C(1)–C(6)	1.403	1.392	C(2)–C(1)–C(6)	117.7	119.1
C(1)–C(7)	1.396	1.392	C(6)–O(8)–H(9)	104.5	
C(6)–H(8)		1.084	C(2)–C(1)–C(7)	122.2	121.6
C(6)–O(8)	1.376		C(6)–C(1)–C(7)	120.2	119.2
O(8)–H(9)	0.996		H–N–C		111.0
C–N		1.438	C(2)–C(1)–C(6)–H(8)		359.9
N–H		1.028	C(2)–C(1)–C(6)–O(8)	0.0	
a	1.405	1.381	O(4)–C(2)–C(1)–C(6)	179.9	180.3
b	1.376	1.396	O(3)–C(2)–C(1)–O(4)	180.0	179.9
c	1.398	1.396	H–N–C–C		±31.6

Table 2. STO-3G-optimized geometrical parameters of transition states for the uncatalysed salicylic (SA) and *p*-aminobenzoic (PABA) acid decarboxylation reactions (bond lengths in Å; bond and torsion angles in degrees)

Parameter	SA	PABA	Parameter	SA	PABA
C(1)–C(2)	1.884	1.887	C(1)–H(5)–O(4)	130.4	131.2
C(2)–O(3)	1.187	1.118	C(2)–O(4)–H(5)	79.9	79.4
C(2)–O(4)	1.304	1.301	C(2)–C(1)–H(5)	58.3	57.8
O(4)–H(5)	1.241	1.243	C(2)–C(1)–C(6)	116.6	115.6
C(1)–H(5)	1.307	1.307	C(2)–C(1)–C(7)	114.1	115.6
C(1)–C(6)	1.414	1.412	C(6)–C(1)–C(7)	116.0	115.9
C(1)–C(7)	1.420	1.412	C(6)–O(8)–H(9)	106.3	
C(6)–H(8)		1.087	H–N–C		112.2
C(6)–O(8)	1.384		C(1)–C(2)–O(4)–H(5)	1.2	0.0
O(8)–H(9)	0.989		O(3)–C(2)–C(1)–O(4)	179.4	180.0
C–N		1.427	C(2)–C(1)–C(6)–H(8)		320.7
N–H		1.026	C(2)–C(1)–C(6)–O(8)	318.4	
C(1)–C(2)–O(3)	121.4	120.8	O(4)–C(2)–C(1)–C(6)	108.5	109.8
C(1)–C(2)–O(4)	91.2	91.6	H–N–C–C		±29.8

For each pair of stationary points, the similarity of the salicylic and *p*-aminobenzoic structures is apparent. This close resemblance is quantitatively demonstrated in Tables 1—5. All the geometrical parameters in these Tables are closely similar, except for the bond lengths in the reactant molecules (Table 1). In salicylic acid, these parameters are influenced by the presence of the *ortho*-hydroxy substituent, and by the formation of an intramolecular hydrogen bond between that hydroxy group and the oxygen atom of the carbonyl group. As a result of this, the benzene ring appears to be distorted from hexagonal symmetry. Two of the C–C bond lengths of the ring (*b* and *d* in Figure 1) are significantly shorter than the others. Such an arrangement is in complete agreement with salicylic acid diffraction studies,[24,25] and suggests that the quinonoid structure constitutes the major valence-bond structure contributing to the overall resonance state of the molecule. As for *p*-aminobenzoic acid, the most stable calculated structure corresponds to a non-planar configuration around the nitrogen atom with H–N–C–C torsion angles of ±31.6°. This result might have been expected since it is well known that minimal basis sets, in contrast to split-valence sets, underestimate valence angles at heteroatoms, and hence often exaggerate the degree of non-planarity, in particular at a nitrogen atom.[26,27] In the crystal structure of *p*-aminobenzoic acid, the nitrogen atoms are also significantly non-planar, and the positions of the hydrogen atoms correspond to a configuration about half-way between tetrahedral and planar.[28,29]

Every decarboxylation involves three processes: O–H bond breaking, C–C bond breaking, and C–H bond making. In the uncatalysed concerted mechanism, the geometries of the transition states are depicted by coplanar four-centre structures (Figure 2) in which the breaking of the O(4)–H(5) and C(1)–C(2) bonds proceeds simultaneously with C(1)–H(5) bond formation. In this sense, such structures do not differ from the activated complexes calculated for the decarboxylation of formic, acetic, and carbamic acids.[30–32] However, the main difference lies in the relative positions of the reaction centres. In the present transition states, as well as in that for catalysis by the one water molecule described later, the carboxy (carboxylate) group is moved out of the plane of the benzene ring and rotated around the C(1)–C(2) bond axis in such a way that this group adopts a nearly perpendicular conformation with respect to the rest of the molecule. These two motions, respectively defined by

Table 3. STO-3G-optimized geometrical parameters of transition states for the salicylic (SA) and *p*-aminobenzoic (PABA) acid decarboxylation reactions catalysed by one water molecule (bond lengths in Å; bond and torsion angles in degrees)

Parameter	SA	PABA	Parameter	SA	PABA
C(1)–C(2)	1.881	1.889	O(11)–H(5)–C(1)	164.3	165.9
C(2)–O(3)	1.205	1.206	H(5)–C(1)–C(2)	87.7	86.8
C(2)–O(4)	1.272	1.269	H(10)–O(11)–H(12)	105.6	105.3
C(1)–H(5)	1.276	1.277	C(2)–C(1)–C(6)	109.7	110.7
O(4)–H(10)	1.293	1.295	C(2)–C(1)–C(7)	110.9	110.2
H(10)–O(11)	1.065	1.063	C(6)–C(1)–C(7)	115.1	115.0
O(11)–H(5)	1.230	1.228	C(6)–O(8)–H(9)	106.4	
O(11)–H(12)	0.982	0.983	H–N–C		112.4
C(1)–C(6)	1.420	1.420	H(5)–C(1)–C(2)–O(4)	350.2	2.6
C(1)–C(7)	1.431	1.420	O(3)–C(2)–C(1)–O(4)	180.6	179.6
C(6)–H(8)		1.087	C(2)–O(4)–H(10)–O(11)	356.3	5.7
C(6)–O(8)	1.380		O(4)–H(10)–O(11)–H(5)	358.5	357.2
O(8)–H(9)	0.989		H(10)–O(11)–H(5)–C(1)	350.5	358.5
C–N		1.424	O(11)–H(5)–C(1)–C(2)	14.5	0.7
N–H		1.026	H(12)–O(11)–H(10)–O(4)	106.4	104.3
C(1)–C(2)–O(3)	110.4	109.5	C(2)–C(1)–C(6)–H(8)		304.9
C(1)–C(2)–O(4)	111.3	112.1	C(2)–C(1)–C(6)–O(8)	304.3	
C(2)–O(4)–H(10)	111.4	111.3	O(4)–C(2)–C(1)–C(6)	104.8	117.7
O(4)–H(10)–O(11)	157.4	157.4	H–N–C–C		±29.7
H(10)–O(11)–H(5)	86.6	86.3			

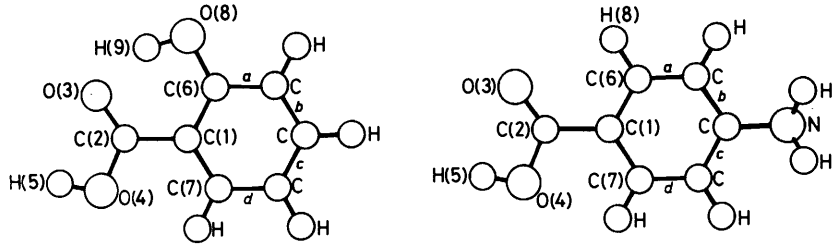

Figure 1. ORTEP Plots of salicylic and *p*-aminobenzoic acids

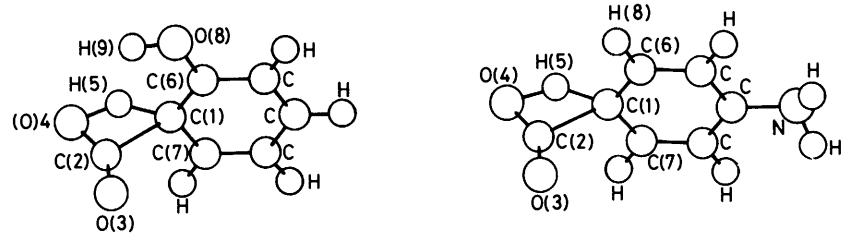

Figure 2. ORTEP Plots of the uncatalysed transition states for thermal decarboxylation of salicylic and *p*-aminobenzoic acids

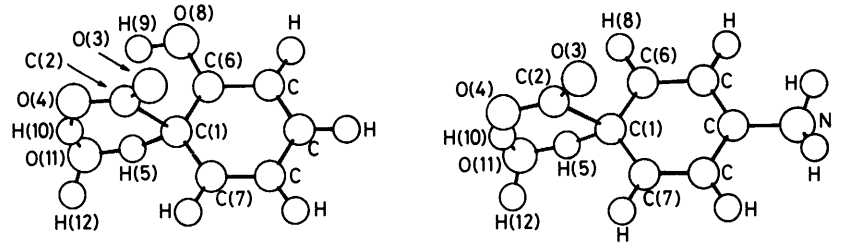

Figure 3. ORTEP Plots of the transition states with catalysis by one water molecule for thermal decarboxylation of salicylic and *p*-aminobenzoic acids

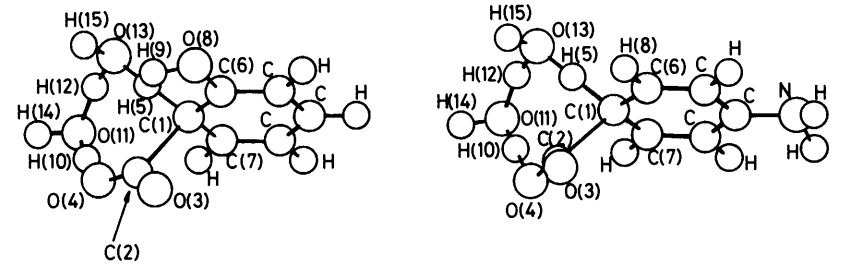

Figure 4. ORTEP Plots of the transition states with catalysis by two water molecules for thermal decarboxylation of salicylic and *p*-aminobenzoic acids

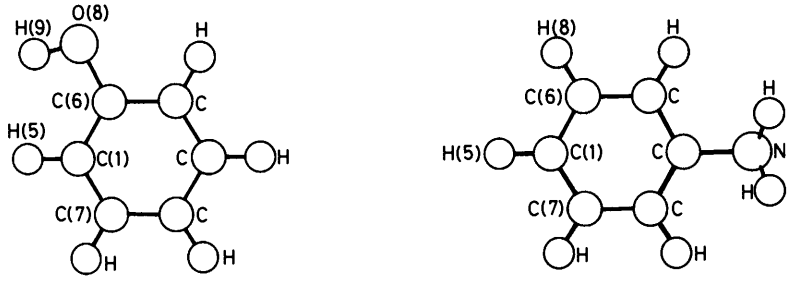

Figure 5. ORTEP Plots of the phenol and aniline molecules

Table 4. STO-3G-optimized geometrical parameters of transition states for the salicylic (SA) and *p*-aminobenzoic (PABA) acid decarboxylation reactions catalysed by two water molecules (bond lengths in Å; bond and torsion angles in degrees)

Parameter	SA	PABA	Parameter	SA	PABA
C(1)–C(2)	1.898	1.893	H(12)–O(13)–H(5)	101.7	101.4
C(2)–O(3)	1.210	1.209	O(13)–H(5)–C(1)	172.1	173.5
C(2)–O(4)	1.250	1.255	H(5)–C(1)–C(2)	93.7	88.5
C(1)–H(5)	1.298	1.289	H(14)–O(11)–H(10)	104.9	104.7
O(4)–H(10)	1.390	1.385	H(15)–O(13)–H(12)	106.8	106.8
H(10)–O(11)	1.027	1.030	C(2)–C(1)–C(6)	113.4	113.6
O(11)–H(12)	1.280	1.292	C(2)–C(1)–C(7)	106.8	108.4
H(12)–O(13)	1.069	1.064	C(6)–C(1)–C(7)	114.5	114.7
O(13)–H(5)	1.212	1.226	C(6)–O(8)–H(9)	105.8	
O(11)–H(14)	0.981	0.981	H–N–C		112.2
O(13)–H(15)	0.982	0.982	H(5)–C(2)–C(1)–O(4)	39.2	65.5
C(1)–C(6)	1.425	1.422	O(3)–C(2)–C(1)–O(4)	179.9	178.2
C(1)–C(7)	1.422	1.413	C(2)–O(4)–H(10)–O(11)	297.1	309.3
C(6)–H(8)		1.087	O(4)–H(10)–O(11)–H(12)	22.0	40.7
C(6)–O(8)	1.383		H(10)–O(11)–H(12)–O(13)	11.3	14.3
O(8)–H(9)	0.988		O(11)–H(12)–O(13)–H(5)	21.5	12.1
C–N		1.427	H(12)–O(13)–H(5)–C(1)	59.3	57.0
N–H		1.026	O(13)–H(5)–C(1)–C(2)	245.8	246.3
C(1)–C(2)–O(3)	108.2	109.2	H(14)–O(11)–H(10)–O(4)	265.6	283.1
C(1)–C(2)–O(4)	112.8	111.4	H(15)–O(13)–H(12)–O(11)	266.7	258.4
C(2)–O(4)–H(10)	130.7	123.7	C(2)–C(1)–C(6)–H(8)		306.1
O(4)–H(10)–O(11)	165.9	167.7	C(2)–C(1)–C(6)–O(8)	302.5	
H(10)–O(11)–H(12)	97.3	98.6	O(4)–C(2)–C(1)–C(6)	157.7	180.7
O(11)–H(12)–O(13)	163.5	163.4	H–N–C–C		±30.0

Table 5. STO-3G-optimized geometrical parameters of phenol, aniline, and carbon dioxide molecules (bond lengths in Å; bond and torsion angles in degrees)

Parameter	Phenol	Aniline	Parameter	Phenol	Aniline
C(1)–H(5)	1.082	1.081	H(5)–C(1)–C(6)	119.7	120.3
C(1)–C(6)	1.392	1.386	C(6)–C(1)–C(7)	119.8	119.3
C(1)–C(7)	1.386	1.386	C(6)–O(8)–H(9)	105.3	
C(6)–H(8)		1.083	H–N–C		110.4
C(6)–O(8)	1.395		H(5)–C(1)–C(6)–H(8)		360.0
O(8)–H(9)	0.989		H(5)–C(1)–C(6)–O(8)	0.0	
C–N		1.444	H–N–C–C		±32.4
N–H		1.028	C=O (CO_2)	1.188	

Table 6. Differences of some bond lengths (Å) between the uncatalysed transition states and the stable reactant (R) or product (P) molecules

Molecule	$\Delta C(1)C(2)^R$	$\Delta C(1)H(5)^P$	$\Delta O(4)H(5)^R$
Benzoic acid [10]	0.417	0.251	0.226
Salicylic acid	0.385	0.225	0.251
p-Aminobenzoic acid	0.376	0.226	0.254

the C(2)–C(1)–C(6)–H(8) [O(8)] and O(4)–C(2)–C(1)–C(6) torsion angles, imply a breakdown of coplanarity. This loss of coplanarity, which reduces the resonance interaction of the carboxy group with the benzene nucleus, has two effects. First, it weakens the C(1)–C(2) bond, which is consequently very long (1.9 Å). Secondly, the group is forced into a favourable geometric position. In such structures, the electrophilic hydrogen atom, coming either from the carboxy group itself or *via* proton transfer through a water molecule, is situated in a position where it may readily complex with the field of the π orbital of C(1). Moreover, in the case of salicylic acid, the turning of the carboxy group out of coplanarity also implies the rupture of the intramolecular hydrogen bond if this bond still exists in aqueous solution.[33,34] Thus the O(3)–H(9) distance goes from 1.6 Å in salicylic acid to respectively 3.4 and 3.5 Å in the transition state structures corresponding to no catalysis and catalysis by one water molecule.

Comparison of the two four-centre transition-state structures with that of benzoic acid[10] indicates that 1,3-hydrogen migration is more advanced in the substituted acids than in benzoic acid itself, but the reverse is observed for the breaking of the carbon–carbon bond. This can be deduced from Table 6 which collates the elongations of the C(1)–C(2) and O(4)–H(5) bonds observed in the transition states with respect to their equilibrium values in the reactants, as well as the differences in C(1)–H(5) distances between the transition states and the product molecules. The behaviour of the substituted benzoic acids with respect to the parent compound is consistent with the experimental fact that *ortho*- and *para*-substitution by electron-releasing groups increases both the attraction of the proton by the α-carbon atom and the rate of decarboxylation.

To account for the solvent participation in the decarboxylation reaction in solution, the chosen approach in this work was to consider the solvent not as a medium in which the reaction is carried out, but as an active participant in the chemical process. In this scheme, the aqueous solvent is represented by a discrete number of water molecules, the geometric parameters of which form part of the reaction co-ordinate.

The structures of the transition states involving one water molecule are represented in Figure 3. In each of these structures, the reacting part forms a nearly planar six-membered ring perpendicular to the rest of the molecule. The C(2)–C(1)–C(6)–H(8) [O(8)] and O(4)–C(2)–C(1)–C(6) torsion angles defining the rotation of the carboxylate group amount respectively to 304.4° (304.9°) and 104.8° (117.6°) in salicylic (*p*-aminobenzoic) acid. Table 7 reports the differences in bond lengths involved in the reaction centre with regard to the equilibrium values either in the reactants or in the corresponding products. In comparison with the uncatalysed concerted process, the C(1)–H(5) bond formation is more advanced. This stands out in Tables 6 and 7 where the ΔC(1)–H(5) values are compared. On the other hand, increases in the length of the breaking C(1)–C(2) bond are similar in the uncatalysed mechanism and that with one water molecule. In the latter, however, only one of the two hydrogen shifts is

Table 7. Differences of some bond lengths (Å) between the transition states with catalysis by one water molecule and the stable reactant (R), water (W), or product (P) molecules

Molecule	$\Delta C(1)C(2)^R$	$\Delta C(1)H(5)^P$	$\Delta O(4)H(10)^R$	$\Delta H(10)O(11)^W$	$\Delta O(11)H(5)^W$
Benzoic acid [10]	0.427	0.223	0.389	0.065	0.206
Salicylic acid	0.382	0.194	0.303	0.076	0.241
p-Aminobenzoic acid	0.378	0.196	0.306	0.074	0.239

Table 8. Differences of some bond lengths (Å) between the transition states with catalysis by two water molecules and the stable reactant (R), water (W), or product (P) molecules

Parameter	Benzoic acid [10]	Salicylic acid	*p*-Aminobenzoic acid
$\Delta C(1)C(2)^R$	0.424	0.399	0.382
$\Delta C(1)H(5)^P$	0.252	0.216	0.208
$\Delta O(13)H(5)^W$	0.185	0.223	0.237
$\Delta H(12)O(13)^W$	0.090	0.080	0.075
$\Delta O(11)H(12)^W$	0.270	0.291	0.303
$\Delta H(10)O(11)^W$	0.039	0.038	0.041
$\Delta O(4)H(10)^R$	0.397	0.400	0.396

effected at the transition state, *i.e.* the carboxylic hydrogen H(10) is almost fully transferred to the water molecule. The second hydrogen transfer, of H(5) from water to C(1), is only half complete.

Looking now at the transition states of salicylic and *p*-aminobenzoic acids in the presence of two water molecules, we can see (Figure 4) that they are represented by non-planar eight-membered rings. In these structures, the number of atoms involved in the reaction centre is, at present, large enough for the carboxy group no longer to need to be perpendicular to the benzene ring; thus its proton, after transfer through the chain of the water molecules, can approach C(1) in a suitable geometrical way. The distance variations summarized in Table 8 indicate that, in these transition states, two out of the three hydrogen transfers are nearly complete: H(10) moves towards O(11) and H(12) towards O(13). The third one, the transfer of H(5) from one of the water molecules to C(1), is proceeding, but to a greater extent in the two aforementioned acids than in benzoic acid. This behaviour reflects the magnitude of the charge carried in the reactants by the α-carbon atom, which is enhanced by the presence of the electron-releasing substituents *ortho* and *para* to the carboxy group. At the 3-21G//STO-3G level of calculation, the C(1) charges are, respectively, −0.245, −0.296, and −0.273e in benzoic, salicylic, and *p*-aminobenzoic acids. Finally, it is interesting that the H(5) moves in a straight line between O(13) and C(1) [C(1)–H(5)–O(13) = 172°], as in a normal hydrogen bond. The introduction of two water molecules has thus suppressed all the angle strains existing in the previous planar smaller-ring transition-state structures.

To conclude, it can be said that in aqueous solution (*a*) the species of salicylic or *p*-aminobenzoic acid which undergoes decarboxylation is the free acid; (*b*) the α-protonated form of the carboxylate anion constitutes the transition state, arising from the progressive reorganization of the chain of water molecules through which the carboxylic hydrogen atoms is transferred, and the carbon–carbon bond is greatly elongated; and (*c*) with regard to the three processes involved in the decarboxylation reaction, the proposed mechanism corresponds to an asynchronous concerted process. All attempts to find the σ-complex intermediate postulated by the experimentalists have failed.

Table 9 reports the total energies of the isolated molecules and the relative energies of both the activation barriers and the heats of reaction. All the relative values are given in kcal mol^{-1} with respect to the isolated reactant, *i.e.* salicylic or *p*-aminobenzoic acid, in some cases with one or two water molecules.

Table 9. Total (a.u.) and relative (kcal mol^{-1})[a] energies for salicylic and *p*-aminobenzoic acid decarboxylation

Reaction	System	STO-3G// STO-3G	3-21G// STO-3G
p-Aminobenzoic acid	$H_2NC_6H_4CO_2H$	−467.306 13	−470.706 00
	$C_6H_5NH_2$	−282.212 73	−284.135 89
	CO_2	−185.068 39	−186.557 03
	H_2O	−74.965 90	−75.583 69
	Activation barrier		
		114.3	99.1
	$+1H_2O$	74.0	61.9
	$+2H_2O$	58.4	37.3
	Heat of reaction	15.7	8.2
Salicylic acid set 1	$HOC_6H_4CO_2H$	−486.834 04	−490.436 03
	C_6H_5OH	−301.733 04	−303.857 09
	Activation barrier		
		118.9	105.9
	$+1H_2O$	78.4	67.7
	$+2H_2O$	64.4	46.2
	Heat of reaction	20.5	13.7
Salicylic acid set 2	$HOC_6H_4CO_2H$	−486.817 47	−490.413 87
	Activation barrier		
		110.6	94.3
	$+1H_2O$	71.0	57.8
	$+2H_2O$	55.9	33.4
	Heat of reaction	10.1	−0.2

[a] 1 kcal = 4.184 kJ.

In the case of salicylic acid, two sets of values are reported, corresponding respectively to internally hydrogen-bonded or non-hydrogen-bonded structures. In the first set, the values were obtained from the optimized structures depicted in Figures 1—5. The second set were calculated by keeping the structure of each of the stationary points at their optimized geometries constant, except for the position of H(9) which, in all cases, was rotated by 180° around the C(6)–O(8) phenolic bond, and for which the C(6)–O(8)–H(9) valence angle was arbitrarily fixed at 110°. The reason for this is that, in the first set of relative values, the reactant is stabilized by the intramolecular hydrogen bond, which no longer exists in the uncatalysed or catalysed transition state structures; lack of this correction would lead to overestimated activation energies. In fact, in aqueous solution, two types of behaviour are possible: either the intramolecular hydrogen bond still exists in the free salicylic acid and is then changed into one or more intermolecular hydrogen bonds in the transition structures (these have not been taken into account in this work), or else the intramolecular hydrogen bond of salicylic acid is destroyed in aqueous solution in deference to intermolecular hydrogen bonds with the solvent and thereafter everything happens in a similar way for the reactant and the transition states. It is difficult to account for the solvation effect, which would imply a larger number of water molecules; the relative values given in the second set are thought to be more realistic since in this case, all structures share the same error,

Table 10. Experimental activation energies (kcal mol^{-1})[a]

System	Solvent	E_a	Ref.
Salicylic acid	Catechol	22.9	20
	Benzoic acid	29.9	21
	Resorcinol	33.6	2
	Quinoline	34.7	22
	Glycerol	38.7	18
	(Molten state)	43.0	23
p-Aminobenzoic acid	Glycerol	19.9	18
	Catechol	22.0	19
	Water	22.8	15

[a] 1 kcal = 4.184 kJ.

i.e. no extra stabilization due to intra- or inter-molecular interactions.

For comparison, the experimental activation energies obtained in various solvents are given in Table 10. Hitherto, no value has been reported for the decomposition of salicylic acid in aqueous solution. Thus, although no firm conclusion can be inferred about the proposed mechanism, the calculated activation energy of 33.4 kcal mol^{-1}, falling within the range of the experimental values, makes this mechanism likely. This inference is supported by the decrease in activation energies *vs.* the successive substitution of hydroxy groups into the *ortho*- and *para*-positions of benzoic acid. The values obtained for the decarboxylation of benzoic acid,[10] salicylic acid, and *p*-hydroxysalicylic acid,[35] respectively 44.1, 33.4, and 28.8 kcal mol^{-1}, closely approach the experimental values measured in resorcinol solution, *i.e.* >39.0, 33.6, and 29.2 kcal mol^{-1}.[2] Although the absolute values may be different in aqueous solution, the observed decrease in activation energies clearly reflects the substitution effect caused by the electron-releasing groups, which increase the electron density on the carbon atom next to the carboxy group. At the 3-21G//STO-3G level of calculation, the charge borne by this atom amounts, respectively, to −0.245, −0.296, and −0.316e in the three acids mentioned. Thus it can be concluded that the decarboxylation reaction is at least partly controlled by the attraction of the proton to the α-carbon atom. This is in good agreement with the geometrical description of the transition-state structures given here.

For *p*-aminobenzoic acid the computed activation energy of 37.3 kcal mol^{-1} is much higher than any experimental value given in Table 10. However, in view of the charge borne by C(1) (−0.273e), the activation barrier corresponding to the process catalysed by two water molecules fits in which the previous relation found between the activation energy and the charge on C(1). The discrepancy between the theoretical and experimental results could be ascribed to the nature of the decarboxylating species. In fact, the mechanism of decarboxylation of acids containing an amino substituent is further complicated by the possibility of protonation of the substituent and by the fact that the acid can exist as ampholite or zwitterion.

Finally, Table 9 shows that the addition of successively one and two water molecules in the reaction mechanism decreases the activation energy by respectively 37 and 24 kcal mol^{-1}. It is thus clear that there is no convenient intramolecular route for proton transfer from the carboxy group to the aromatic ring. The protonation, which is part of the decarboxylation reaction, is accomplished by transfer from the acid molecule through the solvent molecules. Thus the solvent behaves as a real catalyst as well as fulfilling its solvation role, and its participation as proton relay becomes essential in the understanding of the decarboxylation reaction.

Conclusion

With the intention of elucidating the decarboxylation mechanism of aromatic carboxylic acids substituted by electron-donating groups in *ortho*- and *para*-positions, reaction pathways in aqueous solution have been calculated for the decomposition of salicylic and *p*-aminobenzoic acids. In these reactions, the solvent is represented by a discrete number of water molecules. Their catalytic action, as proton relay, gives them an active part in the decarboxylation mechanism. Furthermore, since no intermediate was found along the reaction pathway, the mechanism proposed is a concerted process in which the C–C bond breaking and the transfer of the carboxylic hydrogen atom through the solvent molecules to the α-carbon atom take place simultaneously. In comparison with benzoic acid decarboxylation, the presence of *ortho*- and *para*-electron-releasing substituents on the aromatic ring increases the electron density on the carbon atom next to the carboxy group, and therefore facilitates the approach of the proton. Finally, with regard to the decarboxylation mechanisms postulated by experimentalists, except for the fact that it is not a two-step process, the pseudo-unimolecular decomposition of the acid by interaction with a chain of water molecules agrees with the calculations. From a theoretical point of view, as shown in a preceding paper,[10] the kinetically equivalent bimolecular attack of a solvated proton on the α-carbon of the anion of the acid must be discarded, since it leads to unreliable activation energies.

Acknowledgements

This work is part of a project funded by the Swiss National Foundation for Scientific Research. The author gratefully acknowledges the generous assistance of the Centre de Calcul de l'Ecole Polytechnique Fédérale de Lausanne.

References

1 H. Schenkel and M. Schenkel-Rudin, *Helv. Chim. Acta*, 1948, **31**, 514.
2 B. R. Brown, D. H. Hammick, and A. J. B. Scholefield, *J. Chem. Soc.*, 1950, 778.
3 A. V. Willi, *Chimia*, 1961, **15**, 239.
4 G. S. Pande, *J. Sci. Ind. Res.*, 1967, **26**, 393.
5 J. W. Wilt, *J. Org. Chem.*, 1956, **21**, 920.
6 D. Trivich and F. H. Verhoek, *J. Am. Chem. Soc.*, 1943, **65**, 1919.
7 K. R. Lynn and A. N. Bourns, *Chem. Ind. (London)*, 1963, 782.
8 A. N. Bourns, *Trans. Roy. Soc. Can., Sect. 4*, 1964, **2**, 277.
9 G. E. Dunn, *Isot. Org. Chem.*, 1977, **3**, 1.
10 P. Ruelle, *J. Comput. Chem.*, in the press.
11 R. A. Poirier and M. A. Peterson, Program MONSTERGAUSS, University of Toronto, 1981.
12 W. J. Hehre, R. F. Stewart, and J. A. Pople, *J. Chem. Phys.*, 1969, **51**, 2657.
13 M. J. D. Powell, Program VAO5AD, Harwell Subroutine Library, Atomic Energy Research Establishment, Harwell, U.K.
14 J. S. Binkley, J. A. Pople, and W. J. Hehre, *J. Am. Chem. Soc.*, 1980, **102**, 939.
15 A. V. Willi, *Z. Phys. Chem. (Frankfurt)*, 1961, **27**, 221.
16 A. V. Willi and P. Vilk, *Z. Phys. Chem. (Leipzig)*, 1968, **59**, 189.
17 J. M. Los, R. F. Rekker, and C. H. T. Tonsbeek, *Recl. Trav. Chim. Pays-Bas*, 1967, **86**, 622.
18 D. Sitamanikyam and E. V. Sundaram, *Ind. J. Chem.*, 1972, **10**, 1011.
19 M. A. Haleem and M. A. Hakeem, *J. Ind. Chem. Soc.*, 1977, **54**, 521.
20 M. A. Haleem, M. A. Hakeem, and J. Salaman, *Muslim Sci.*, 1976, **5**, 109.
21 W. W. Kaeding, *J. Org. Chem.*, 1964, **29**, 2556.
22 G. E. Dunn, E. G. Janzen, and W. Rodewald, *Can. J. Chem.*, 1968, **46**, 2905.
23 L. W. Clark, *Reakts. Sposobn. Org. Soedin.*, 1967, **4**, 599.
24 M. Sundaralingam and L. H. Jensen, *Acta Crystallogr., Sect. B*, 1965, **18**, 1053.

25 G. E. Bacon and R. J. Jude, *Z. Kristallogr.*, 1973, **138**, 19.
26 N. R. Carlsen, L. Radom, N. V. Riggs, and W. R. Rodwell, *J. Am. Chem. Soc.*, 1979, **101**, 2233.
27 S. Saebø and L. Radom, *J. Mol. Struct., Theochem.*, 1982, **89**, 227.
28 T. F. Lai and R. E. Marsh, *Acta Crystallogr.*, 1967, **22**, 885.
29 M. Alleaume, G. Salas-Ciminago, and J. Decap, *C.R. Seances, Acad. Sci., Ser. C*, 1966, 262, 416.
30 P. Ruelle, U. W. Kesselring, and Hô Nam-Tran, *J. Am. Chem. Soc.*, 1986, **108**, 371.
31 P. Ruelle, *Chem. Phys.*, in the press.
32 P. Ruelle, U. W. Kesselring, and Hô Nam-Tran, *J. Mol. Struct., Theochem.*, 1985, **124**, 41.
33 G. E. Dunn and F. L. Kung, *Can. J. Chem.*, 1966, **44**, 1261.
34 J. C. Dearden and Mrs. G. M. Bresnen, *J. Pharm. Pharmacol.*, 1981, **33** (suppl.), 1075.
35 P. Ruelle, unpublished work.

Received 21*st April* 1986; *Paper* 6/766